Packaging investigation and study for optical interfacing of micro components with optical fibers – Part I

Jose Mireles Jr.*, Maribel Gómez, Miguel A. Garcia
Centro de Investigación en Ciencia y Tecnología Aplicada (CICTA) de la Universidad Autónoma de Ciudad Juárez
Ave. Del Charro 450 N., Cd. Juárez Chih. MEXICO, CP 32310
(Recibido: 17 de diciembre de 2006; Aceptado: 10 de febrero de 2007)

An investigation study concerning optical fiber alignment and micro-mirror performance in MOEMS devices is being reviewed in this paper. The central attention of the study is the analysis of optical fibers positioning, alignment, bonding, optical improvements, coupling to micro-lenses for beam collimation and waveguides. Also, we highlight features concerning coupling of optical fibers to micro-mirrors while searching for the proper alignment and characterization of the optical beam reflection, its tolerances, relative positioning, and attachment techniques.

Keywords: MicroElectroMechanical Systems (MEMS); Packaging; Optical interconnects; OptoElectronics

1. Introduction

The encapsulation of MEMS optical devices is a big concern due that it usually represents around 70% of the total cost of the development / manufacturing of microsystem devices [1]. The quest towards the identification of cheaper and less costly encapsulation solutions are key for the release of new electronic products end services needing optimized and cost effective solutions [1-3]. In addition, a key pitfall in taking a semiconductor or MEMS devices from prototype to manufacturing would be the poor selection of attachment materials of interconnected layers, specially the encapsulation layers of the design [4]. This pitfall is commonly found in research institutions wanting to demonstrate a proof-of-concept prototype, where teams are not constrained by manufacturing issues. At prototype development stages, the device assembly configuration is often not revised in detail with regard to selections of attachment methods of interface layers of semiconductor and MEMS designs. Usually, the attachment / bonding methods may be determined by the chosen outsource manufacturer's capabilities without assessment of optimal interfacing in designs. This work presents a summary of an investigation study concerning attachment methods, materials, processes and assembly procedures to specifically attach photonic MEMS devices, including optical fibers into complete electronic devices.

The content of this review paper is presented as follows. The first section considers general methods and processes for aligning and attaching optical fibers to a substrate, which considers direct aligning into silicon substrate, alignment through microlenses, connectors, optical waveguides, and hybrid approaches. Secondly, we address critical issues concerning the development capability to align and package optical fibers with small elements. Issues such as tolerances, lateral and angular misalignments, and attachment methods are considered in this section. The critical issues related to insuring the reliability and stability of packaging over time and temperature are highlighted. The second report (Part II) of this investigation provides a development of alignment and assembly procedures of fiber optic assembly into Silicon chips.

This work was supported by Sandia National Laboratories, contract 9602, PO#659783 January-July 2007 [5].

2. Methods and processes for aligning and attaching optical fibers to a silicon substrate

In this section we present several methods used for aligning

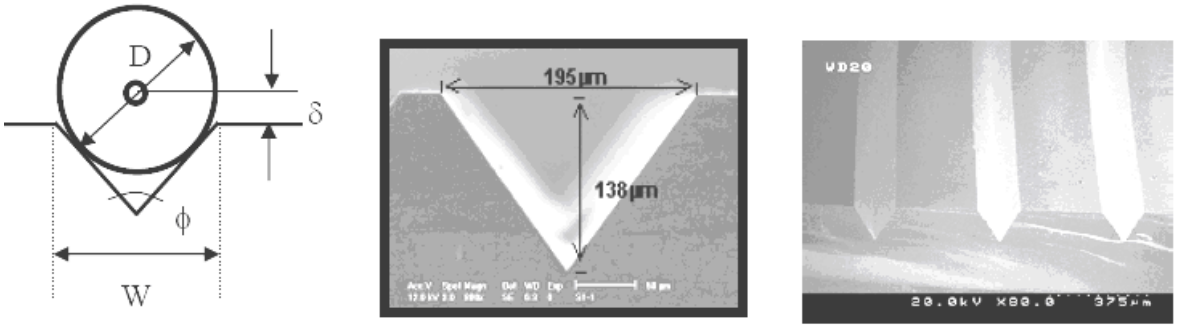

Figure 1.1. Passive Alignment V-groove for holding Optical Fibers [6].

*jmireles@uacj.mx

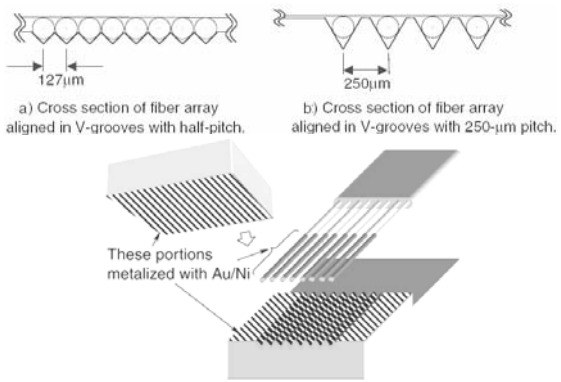

Figure 1.2. Metallized portions of the parts of a fiber array for soldering [6].

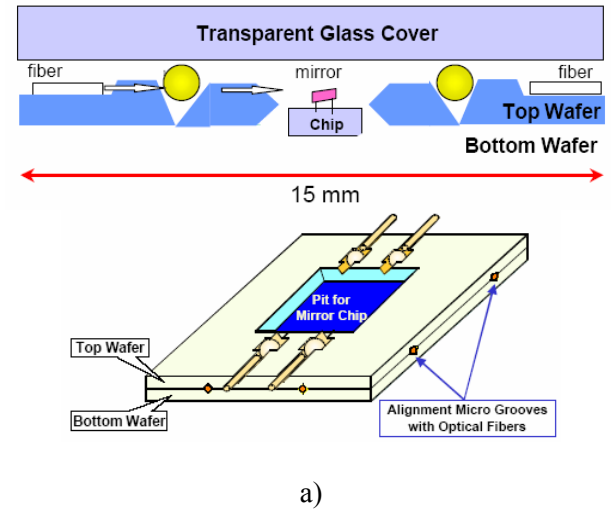

Figure 1.3. a) and b) 2x2 fiber arrangement and mirror die submount [8].

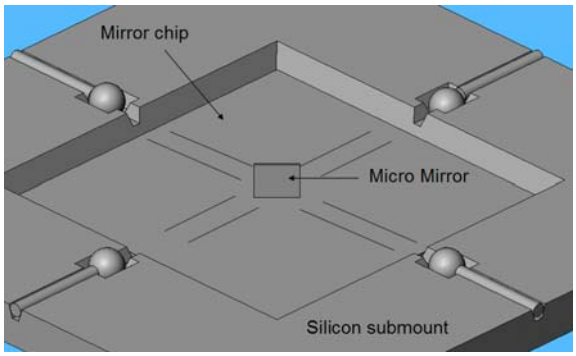

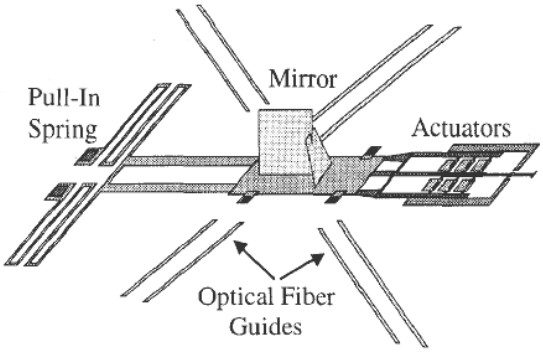

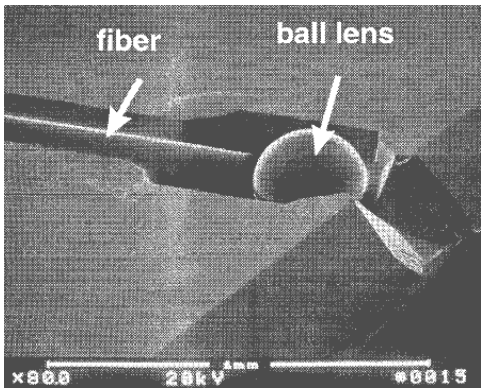

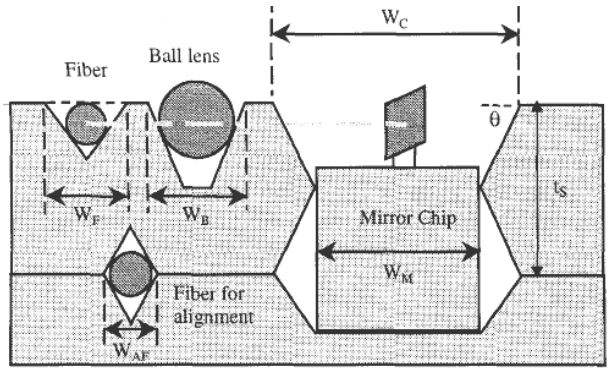

Figure 1.4. 2x2 fiber arrangement and mirror die submount with fiber and ball lens assembly [9].

Table 1. General requirements of epoxy for optical fiber coupling bonding

Optimal viscosity	Several 1,000~10,000 cps
Low shrinkage	<2~3%
Low CTE (by TMA)	~10^{-5}/ºC
Low absorption and excellent durability	
Fast curing and good adhesiveness	

optical fibers with microstructures. Generally, there exist techniques for holding optical fibers to the substrate, through the use of connectors, microlenses, optical waveguides, and hybrid solutions (combining several of the earlier.) We next present several techniques proposed by several research groups divided for each of the general categories.

2.1 Direct alignment and attachment of optical fibers to a silicon substrate

- N. Hori in his chapter "Optical Fiber Jisso Technology" from book [6], provides a review of techniques for aligning and fixing parallel optical fibers to substrates. The standard way to hold optical fibers to the substrate is through using V-grooves. Figure 1.1 shows the standard V-groove micromachined over Silicon (100) substrates.
For the fixing methods of optical fiber arrays shown in figure 1.1, adhesives are generally used to hold the optical fibers to the V-grooves (usually, adhesives are placed in between the V-grooves, top substrate, and fibers.) However, adhesives can not be used in applications requiring hermetic packages; neither in high-temperature applications due to reliability issues (Section 2.3 covers considerations and problems regarding the use of epoxies and adhesives in photonics packaging.) If hermetic packaging is required, metal deposition and soldering (including laser soldering) is often used in conjunction to V-grooves. Figure 1.2 shows V-grooves, as well as optical fibers metallized for soldering attach. Reference [7] shows an study of different metallization options considering low temperature lead Pb-free soldering in V-grooves, which study is summarized in section 2.4 (solder attachment.)
- Lee *et al* in [8], and Huang *et al* in [9] present the alignment of four optical fibers in a 2x2 MEMS fiber optical switch arrangement. The switch is used in conjunction with vertical torsion mirror devices that are fabricated using silicon surface micromachining processes in a die that is dice cut and attached into a bigger Bulk micromachined substrate which contains V-groves. The V-grooves hold micro lenses and optical fibers to align them to the micromirrors of the central surface micromachined die. This is a hybrid packaging method used to minimize active optical alignment between the mirror chip and the optical fibers. Figures 1.3 shows the proposed approach from [8].
In [8], the optical mirror uses an electrostatic approach to bounce from 0° to 45° (ON-OFF activation.) Also, it is claimed that a 0.1° accuracy is obtained in the fiber alignment. In [9] a different mirror structure is introduced for the same submount assembly approach (2x2 switch). However, in [9], the provided approach uses only one micromirror to switch the direction of the optical communication channel, as shown in figure 1.6. In both works, [8] and [9], their approach to align the fibers to the mirrors is by using 300 µm-diameter ball lenses which are droped in the center of a lower wafer containing V-grooves, and an upper wafer which has V-groves on both sides of it. One side servers to align the lower wafer through the V-grooves using dummy fibers, and the other side is used to fix the optical fibers, as shown in figure 1.3-b. However, in their work no further results are reported regarding tolerances, efficiency, or assembly problems.
To diminish power and coupling losses, this assembly scheme uses 300 µm-diameter spherical microlenses. These ball lenses are self assembled in a bulk micromachined micropit as shown in figure 1.4. To fabricate these micropits, mask layout design compensations were used to reduce the convexity of corners due to the extra etching in a (100) silicon die. Also, due to the 12 µm dicing cut error of the central chip, tolerances and dimensions of the mirror should be considered, as well as dimension Wc shown in figure 1.4.
- Abeysinghe *et. al* in [10] propose to use anodic bonding to hold and maintain the optical fibers to V-grooves in the substrate. As a difference of using metallized fibers, or epoxies to hold the fibers, the Silica fibers are coated with a high-Na+ glass (through sputtering of Pyrex, or coating and curing with liquid sodium silicate solution) are placed in a metallized v-groove on the Si submount and anodically bonded, as seen in figure 1.5. This bond has shear strength comparable to solder-bonded components (600 g) and the v-groove autoaligns the fiber to the component in two of the three dimensions. This novel combination of anodic bonding and coated fiber on precision fabricated v-grooves eliminates lenses and packaging time, can lead to lower-cost packages, and will facilitate multicomponent optical submounts and other novel optoelectronic technology.

2.2 Alignment of optical fibers through microlenses

While considering coupling an array of fibers into an opposite array through open space, the light going out of the fibers should be collimated through microlenses [6]. Different types of microlenses are available in the market already. Some of the standard shapes are shown in classifications in table 2 and figure 1.6. Details about different fabrication processes, applications, wafer assembly, and evaluation processes of microlenses are presented in [6]. Example of a GRIN lens structure from [11] shown in figure 1.7. There are different ways to construct microlens using additive, etching, injection, or even ion implantation techniques, discussed in [6].

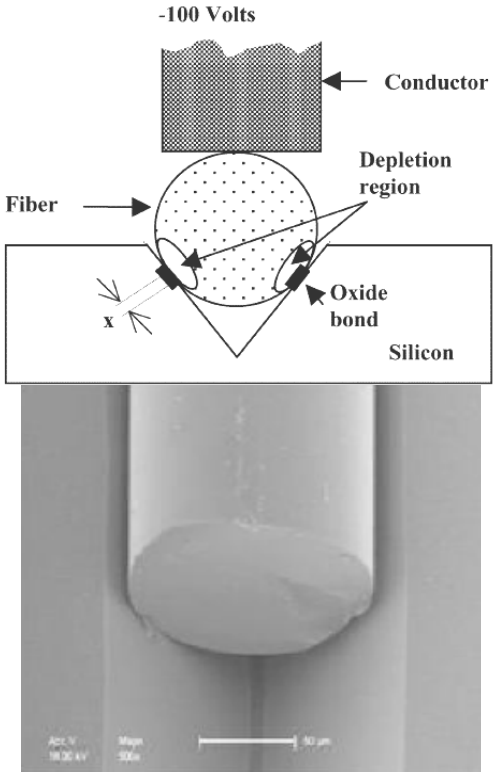

Figure 1.5. Geometry for anodic bonding of silica glass fiber to micromachined v-groove [18].

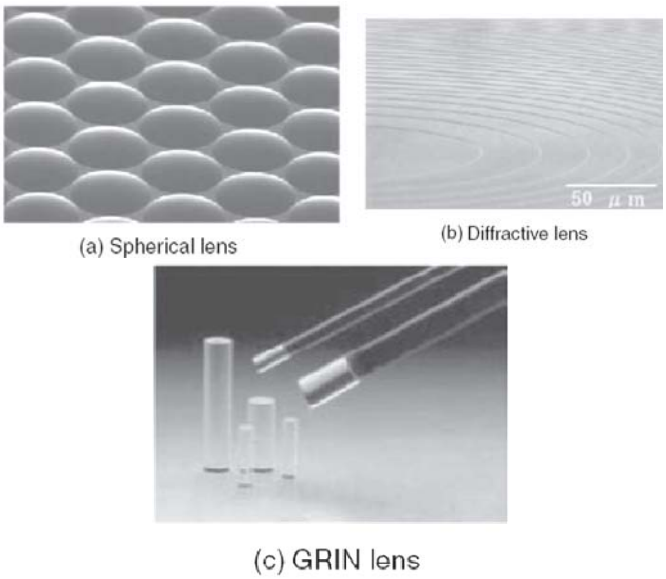

Figure 1.6. Classification of a microlens array structures, from [6].

2.3 Alignment and coupling of optical fibers through waveguides

Several researchers suggest the use of fiber-to-waveguide coupling. This is a very active research today, and the coupling requires small tolerances in assembly and alignment of optical fibers with mirrors, some mirrors embedded in waveguides.

- Glebov *et al*. in [12] propose the use of optical waveguides as a coupling path in between photonic devices for high speed board-to-board optical interconnects. In their system architecture, the photonic devices are placed on PC boards with optical signals that are routed through an optically passive backplane through optical jumpers with MTP connectors. An optical layer consisting on polymer waveguides and 45º reflector micromirrors are embedded in a backplane. The waveguides have propagation losses as low as 0.05 dB/cm at 850 nm, and they are fabricated by direct lithographic patterning. Hot-embossing was also evaluated for the waveguide fabrication resulting in waveguide propagation losses in the range of 0.06-0.1 dB/cm but with poor channel-to-channel uniformity. For the fabrication of the 45º reflector micromirrors, wedge dicing technology was utilized resulting in 0.5 dB losses.

The concept of waveguide utilization is illustrated in figure 1.8. The optical layer contains planar optical waveguides terminated with 45º reflector micromirrors. The planar waveguides are composed of three layers: lower cladding, core, and upper cladding. The refractive index of the core layer is slightly higher than the cladding layers. The typical index difference for multimode waveguide is ~1-3%.

Glebov *et al*. present two general low-cost fabrication methods for waveguides, as shown in figure 1.9. These two techniques use direct lithographic patterning and hot embossing. The photolithographic patterning technologies have better reproducibility and reliability for waveguides manufacturing. For multimode optical waveguides, which ranges core dimensions vary from 20x20 to 50x50μm^2, different photopatternable optical polymers with low absorption at λ=650-980 nm are available on the market. However, depending on the polymer selection for waveguide fabrication, several absorption losses can be obtained. For instance, one can find absorption losses ranging from 0.05dB/cm up to 0.2dB/cm @ 850nm (more details about polymers and losses for different materials in [12].)

A suggested approach to build the 45° reflection micromirrors integrated to waveguides is shown in figure 1.10. In this figure, a simplified fabrication flow of 30x30μm^2 waveguides is shown [12]: (a) The lower cladding and wedge polymer layers are deposited and the wedge base is patterned. The wedge base is accomplished using a mechanical dicing blade v-shaped with 90° angle; (b) One side of the wedge base is tapered to 45º by microdicing and a thin gold (Au) film is deposited on the tapered wedge side; (c) The waveguide core layer is deposited and the channel waveguide is pattered with

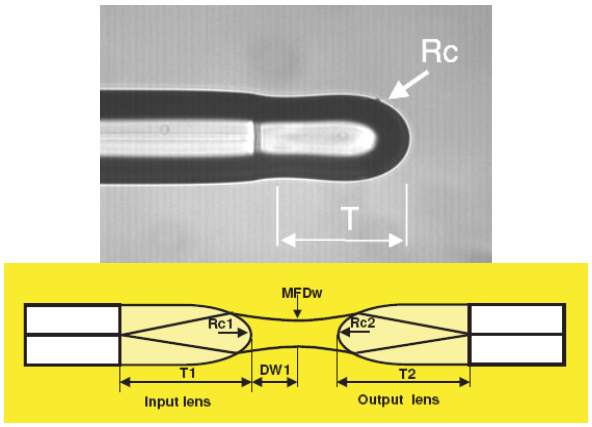

Figure 1.7. SEM Micrograph of a GRIN lens coupled to a fiber, and its collimated lens system [11].

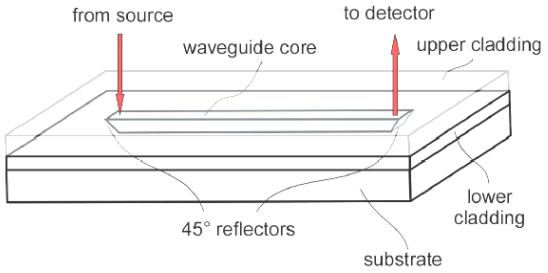

Figure 1.8. Schematic of board optical layer with embedded waveguides and 45° mirrors [12].

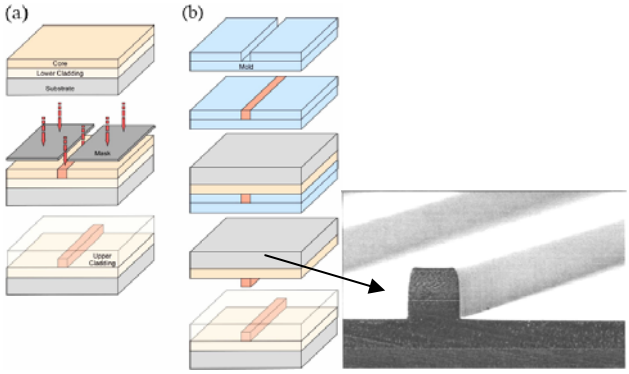

Figure 1.9. Process flows for optical waveguide fabrication using (a) direct lithography and (b) embossing technique with view of a 50x50µm^2 waveguide [12].

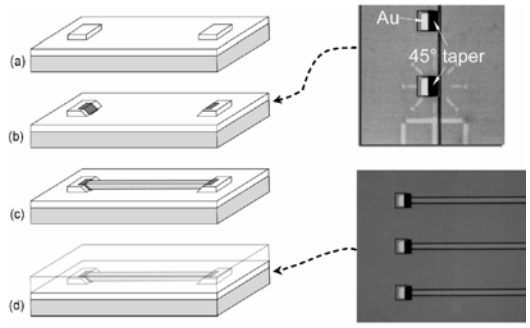

Figure 1.10. Fabrication flow of the embedded polymer waveguides with 45º mirrors formed by wedge dicing technique. The right panels show the top views of the mirror sample at different stages of fabrication [12].

photolithography; (d) The top cladding layer is coated on top of the formed waveguide and mirror structure.

2.4 Hybrid approaches for alignment and coupling of optical fibers

The coupling lighting through optical fibers in [12] was accomplished by combining waveguides, MTP connectors and optical microlenses. The light from the fiber is focused on a 45º micromirror embedded in waveguides by a microlens mounted in the lower subassembly of the adaptor. The microlens adaptor provides possibilities for an easy light mode size reduction and improved alignment tolerances as the light can be focused in a small spot with the diffraction limited size. The microlens adaptors used in [12] have bi-convex silica microlenses with 230 and 120µm radii of curvature (ROC) formed on a 950µm wide silica plate. The microlens lateral dimensions are less than 250µm so that they can accommodate 250µm pitch of the fiber array. The height of the adaptor subassembly is optimized to focus the light on the embedded 45º mirrors and is typically about 200-300µm. Figure 1.11 shows the adaptor subassembly and its cross section drawing.

- A similar proposed scheme to couple optical fibers to waveguides from Karppinen *et al*. in [13] is shown in figure 1.12. Here, two sets of microlenses are used to collimate the optical light coming from VCSELs into micromirrors and into optical waveguides. The required tolerances for their approach were ±10µm, and even if "big" BGA bumps were used for assembly, the microlenses were able to get down to such tolerances of alignment. The emitted wavelength of VCSELs were 850nm. Before proceeding with assembly procedures, simulations were used to calculate the tolerances of the scheme, table 5 shows the list of parameters used in simulations to calculate tolerances of the proposed scheme.
- One hybrid approach was proposed by Bakir et. al in [14], which fabricated and tested microscopic polymer pillars which are used as flexible optical bridge between optical devices and waveguides located in the substrate. Using the polymer Avatrel, polymer pillars are machined using photo-imaging to a height up to 350 µm. The photodefinable polymer Avatrel was used for the fabrication of the optical pillars due to its ease of processing and its unique material properties that include high Tg and low modulus. An evaluation performance of these polymer pillars was accomplished in [14], where the optical coupling efficiency measurements were compared using light source to an optical aperture with and without an optical pillar. For a light source with 12º beam divergence, a 30×150 µm polymer pillar improves the coupling efficiency by 3 to 4.5 dB compared to pillar-free (free-space) optical coupling. Figure 1.13 shows the schematic illustration of mechanical assembly through ball bonding and the optical assembly through the polymer pillars.

The low elastic modulus of the polymer and air cladding of the waveguide contribute to the flexible nature of the

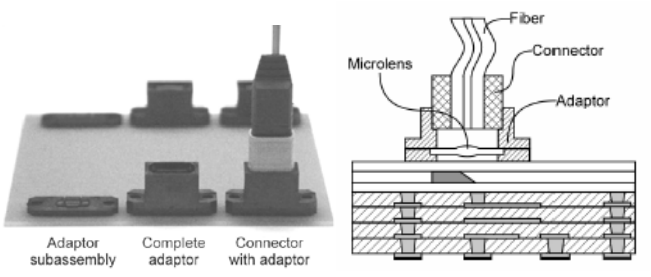

Figure 1.11. Stages of the adaptor / connector assembly, and a drawing of its cross section [12].

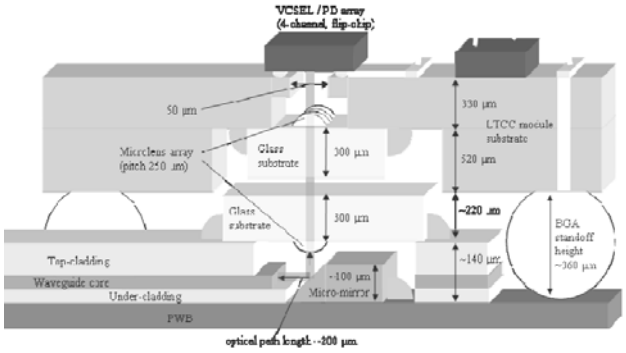

Figure 1.12. Expanded beam created between the two microlens arrays allows alignment accuracy required for BGA assembly of above LTCC substrate [13].

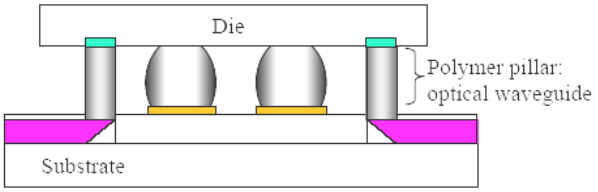

b)

Figure 1.13. Schematic illustration of electrical and optical chip I/O interconnections. An optical bridge (polymer pillar) is used to optically interconnect the chip and the substrate [14].

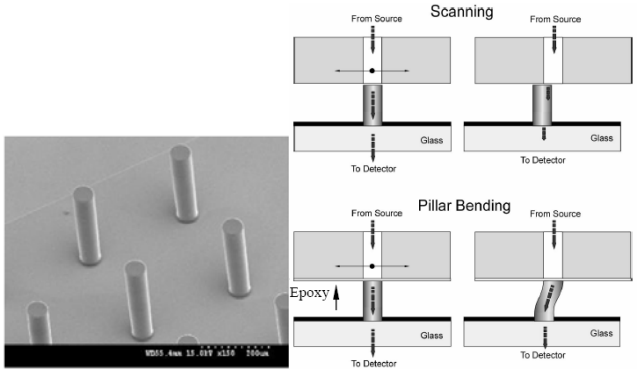

Figure 1.14. a) SEM images of polymer pillars [55 µm diameter, 280 µm tall, 325 µm pitch, ~103/cm2 I/O density], and b) Schematics of the experimental setups used to evaluate the optical displacement compensation of the polymer pillars [14].

polymer pillars. As a result, the lateral misalignment induced by chip-substrate CTE mismatch is compensated by the mechanical compliance of the optical pillars, as shown in figure 1.14.

- Hauffe *et al*. in [15] present a passive alignment coupling of single mode optical fibers with reported coupling losses of 0.7dB. The lower die used in their design use V-grooved structures for optical fiber alignment which are easily micromachined using KOH since they are defined directly by the crystal planes in the Si wafer. Better alignment accuracies in assembles are obtained if alignment ribs are used in the upper die (which have negative profile alignment with respect to the ones located in the lower die,) and the use of flip-chip bonding automation assembly.

So, in [15] a rib height of 4 µm was used. The substrate material used for the ribs was silicon-on insulator (BE-SOI) with a thickness of the silicon top layer of 4 µm (rib height.) Also, they suggested to fabricate both dies in a single wafer process in order to have same etching rates and material thicknesses, as shown in figure 1.16.

Notice in figure 1.16 that the Ti/Au layer is used for bonding purposes and to protect against particles and moisture of the fiber - waveguide interface. The misalignment tolerances of this approach also depends on the following: Since the commercially available wafers have an accuracy of 0.3° at best with a normal distribution, this misalignment accuracy of wafer's real crystal planes with respect to wafers' alignment-axes is unavoidable. So, with an uncertainty of *+/-0.5*° for the angle between crystal axis and v-grooves the error in the groove width is about 1 µm.

3 Critical issues addressing the development capability to align and package optical fibers with elements such micro mirrors

Many coupling issues exist while developing alignment of optical fibers to micromirrors, starting with the obvious optical dispersion of photons in between them, and ending with the assembly and package design tolerances. Below is a list of critical issues found regarding the assembly, alignment and packaging issues involving coupling of optical fibers with micromirrors.

3.1 Non-Understanding Positional Tolerances

Proper understanding of device's optical design is the only way to perform informed decision making on device package design and assembly process. Different erroneous decision making on assembly and alignment problems are associated if specifications are not understood properly, including poor attachment choices, under-tolerances on attachment methods for components that might require high positional tolerance requirements, over specification of tolerances of attachment methods for components requiring lower tolerance requirements can lead to increased costs and to extra assembly process constraints [4].

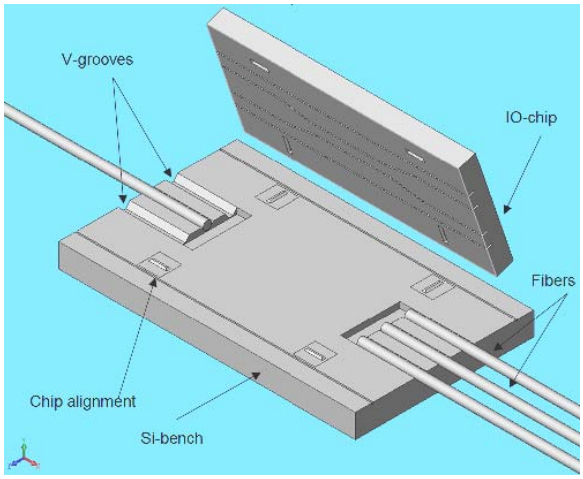

Figure 1.15. Double chip bonding assembly for passive fiber alignment [15].

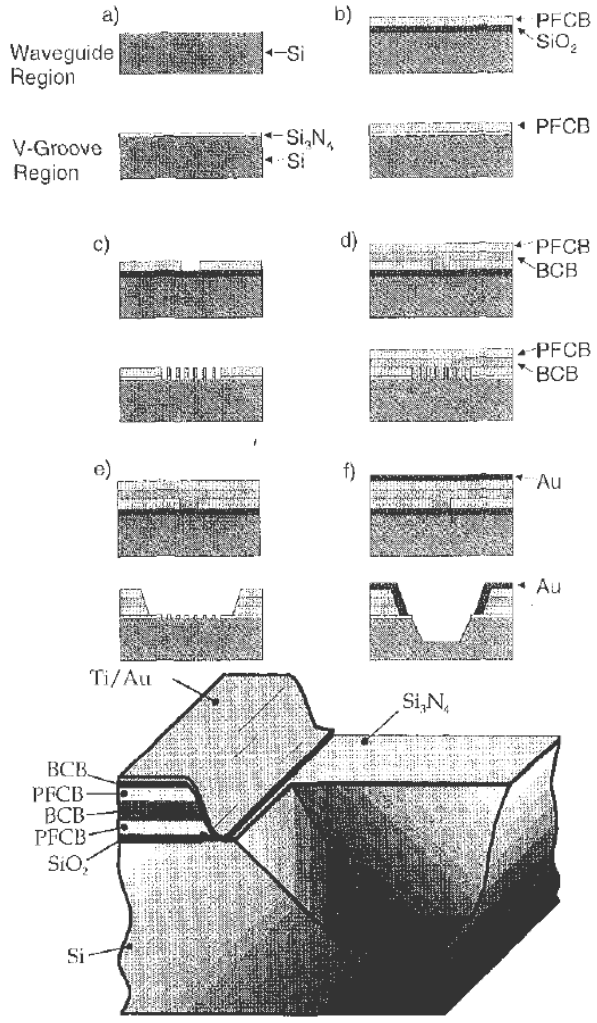

Figure 1.16. Fabrication steps of the single chip approach [15].

Depending on the required tolerances, designers can use low cost solutions (std. pick and place solutions) if requirements for tolerances are 10-20µm, expensive solutions (flip-chip positioning equipment) for 1-5µm required tolerance, or slow and very expensive solutions (usually active alignment required) for tolerances below 1µm [5].

Fiber Misalignment

A study for contact surfaces of multi-fiber optical connectors was presented by Lin in [17]. This study provides preliminaries that are important to be integrated in this investigation concerning orientation and positioning of optical fibers. The results of the study are shown below.

Lateral Misalignment

Optical fibers single-mode applications use light beams that are assumed to have a Gaussian distribution in both step-index and parabolic-index fibers. The loss between two identical fibers is expressed as:

$$L = -10\log\left\{\exp\left[-\left(\frac{d}{w}\right)^2\right]\right\}$$

where d is the lateral misalignment as shown in figure 2.1 (a), and w is the Gaussian spot size. It is required that the insertion loss should be less than 0.5 dB in single-mode MT connectors. Therefore, Lin recommends that the lateral misalignment d may not exceed 3.1µm (assuming the spot size w is equal to the diameter of the single-mode fiber, namely 9µm for single-mode fibers.) This is the reason why MT ferrules accepts a misalignment of 1.5µm to ensure that the tolerance generated by the successive assembly does not affect the performance.

Angular Misalignment

The loss between two identical fibers for single-mode applications, where the light beams are assumed to have a Gaussian distribution in both step-index and parabolic-index fibers can be expressed as:

$$L = -10\log\left\{\exp\left[-\left(\frac{\pi n_2 w\theta}{\lambda}\right)^2\right]\right\}$$

where θ is the angular misalignment as shown in figure 2.1 (b), w is the Gaussian spot size, n_2 is the refractive index of the cladding, and λ is the wavelength of the light. As mentioned before, the insertion loss should be less than 0.5 dB in the general case. Therefore, the angular misalignment θ may not exceed 1.3 deg (when the normalized frequency is 2.4, n_2 is 1.46, and λ is 0.8µm. However, in practical applications, the angular

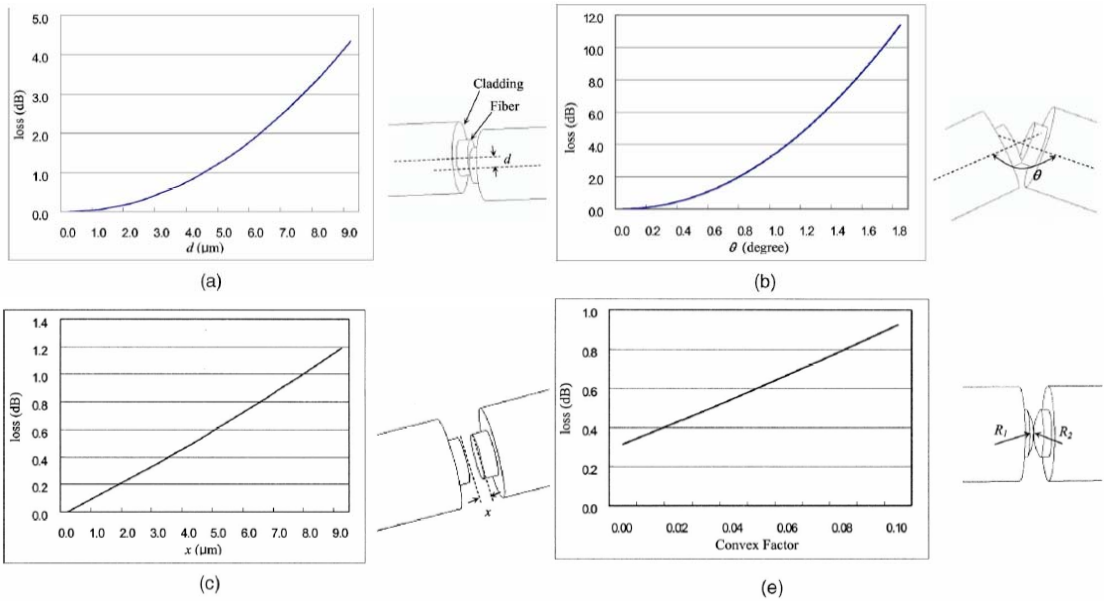

Figure 2.1. Connection losses: (a) lateral misalignment, (b) angular misalignment, (c) separation between fiber ends, (e) convex fiber ends. [17].

misalignment (in connectors) is usually very small (below 0.1 deg) compared to the maximum values. Therefore, the angular misalignment will be neglected here.

Separation Between Fiber Ends

In figure 2.1 (c), where an air gap exists between the fiber ends, there are two boundaries between the fiber medium and the air. Two reflecting surfaces generate about 0.35-dB loss. Therefore, matching grease was used in this study to fill the gap to eliminate the loss. Another loss mechanism is beam divergence owing to the gap between the fiber ends. The loss is given by:

$$L = -10\log\left(1 - \frac{x \cdot NA}{4an_0}\right)$$

where x is the gap distance, a is the core diameter, NA is the numerical aperture of the fiber core, and n_0 is the refractive index of air. For the MT connectors (in his study,) a clip spring was used to eliminate the gap, and matching grease was also applied to the contact surface. Therefore, the assumption was made that losses due to the end separations (in connectors) would not occur.

Convex Fiber Ends

The end faces of the two connecting fibers with radius a are assumed to have radii of curvature R_1 and R_2 as shown in figure 2.1 (e). If $a>>d1$, $d2$, the following relations can be obtained:

$$R_1 \approx \frac{a^2}{2d_1},\ R_2 \approx \frac{a^2}{2d_2}$$

The convexity factor d/a can be defined as

$$\frac{d}{a} = \frac{d_1 + d_2}{a}$$

If the optical wave's angular distribution is uniform, the optical loss can be expressed by:

$$L \approx -10\log\left\{0.93\left[1 - \frac{0.31}{2(2\delta)^{1/2}} \times \frac{d}{a}\right]\right\}$$

where δ is the specific refractive index difference between core and cladding." Since matching grease can be used to fill the gap, the losses owing to convex fiber ends can be neglected.

- Nallani *et al*. in [18] show an analysis of distance tolerances while coupling multimode optical fibers to VCSELs using microlenses consisting of SU-8 (from MicroChem Corporation, Newton, MA) photoresist pedestals having ink-jet-printed polymeric microlenses. The microlenses have a diameter of 120 μm and 30 to 50 μm height (h_i) and which are ink-jet-printed over 80 - 100 μm height (h_p) pedestals with same diameter of 120 μm (see figure 2.2.) A clear advantage of their approach was the use of optical microlens.

3.2 Submounts attachment [16]

In order to maintain optical alignment and device performance, stability of submounts and main components is necessary. The stability can be jeopardized under thermal loads of elevated package temperature environment, TEC operation, and laser diode operation. Design solutions to these thermo-mechanical packaging issues include:

- choice of submount thickness for resistance to thermal gradient warpage;

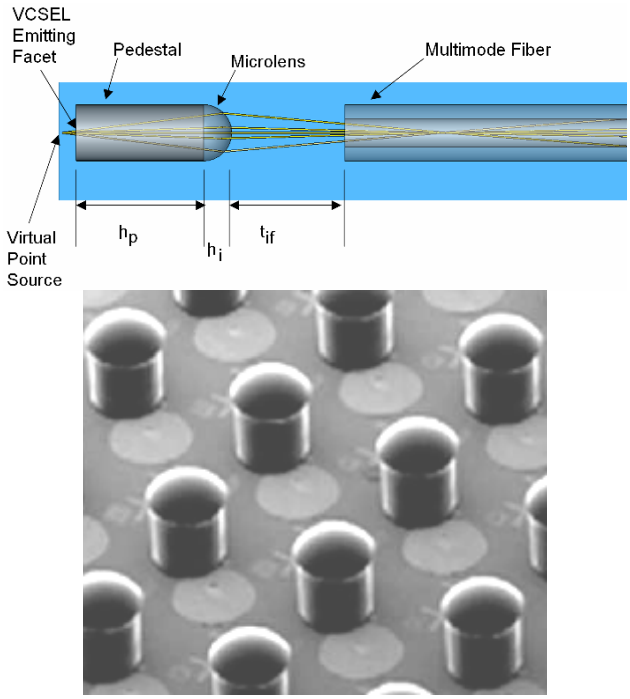

Figure 2.2. Integration process of VCSEL to Optical Fibers using pedestal and microlens printed [18].

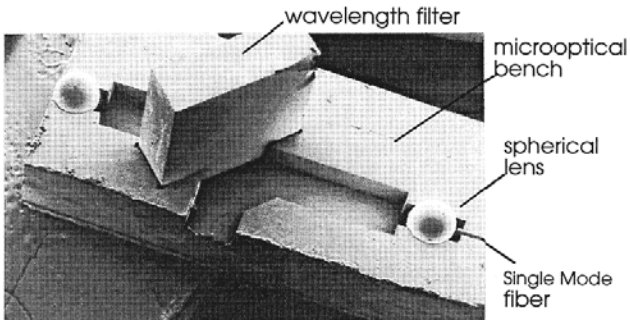

Figure 2.3. Submount alignment of optical fibers through spherical lenses [19].

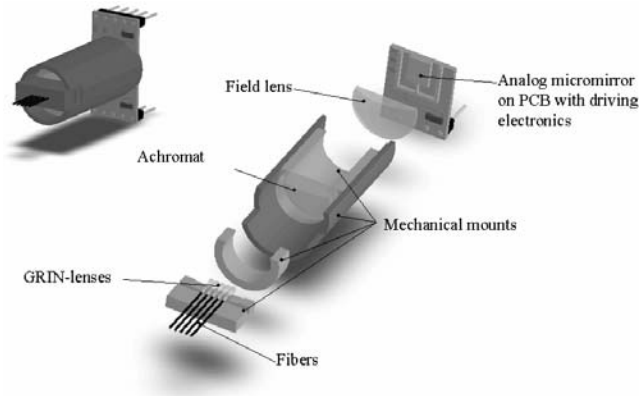

Figure 2.4. Schematic drawing of a switch unit using a MEMS mirror for beam deflection [20].

- proper TEC sizing;
- material selection of submounts for thermal conduction; and
- submount ability to provide temperature uniformity across its surfaces.

- Last decade (by 1996), Gengenbach presented in [19] a submount to hold and align a single mode optical fiber (9/125µm,) two spherical lenses (ϕ 900µm ±5µm,) a wavelength filter (3mm ±50µm x 3mm ±50µm x 1mm ±0.5µm,) a laser diode and a photodiode. The spherical lenses are placed down to ±2µm relative to the bottom of the optical bench, this can be accomplished thanks to the LIGA process submount, as shown in figure 2.3. Small amount of UV-cured epoxy has to be used to fix these spherical optical lenses. The optical fibers are placed in the submount cavity having 1µm wider and deeper shaft. The positioning tolerance is ±50µm close to the spherical lenses.

The important result from this work to our investigation is that even having big tolerances and rough submounts, spherical lenses were able to align optical coupling of 9µm core optical fibers to detectors being several milimeters apart.

- Lausch *et. al* in [20] proposed a fiber optic switch concept using an analog micromirror device, which are coupled through a mechanical submount structure shown in figure 2.4. Losses smaller than 0.4dB were obtained for 0.1 degree misalignment, and 0.5 micron lateral misalignment, thanks to the field lens used in the submount.

- One procedure to create a submount with high numerical aperture (NA) lenses such as that from [20], but using smaller dimmensions is through constructing an array using a three-lens surface scheme [6]. Figure 2.5 shows the structure applied for an optical disk pickup objective lens. The lens diameter was 200 µm, and it had an NA of 0.85. Overall length is 708 µm. The high-NA microlens consists of three lens surfaces. L1 and L2 are convex lenses. L3 is a concave lens filled with a resin with a high refractive index. Substrates and cover glass materials are fused quartz. The refractive index of the resin between L3 and the cover glass was 1.620. The designed tolerances of each surface spacing and optical axis displacement were ±3 µm and ±1 µm, respectively. This structured lens achieved high NA with the 650-nm wavelength design. We conclude from this reference that it is possible to fabricate high-NA microlenses if necessary for demanding applications.

3.3 Epoxy Attachment [16]

The lowest cost attachment material for building photonic devices is epoxy. Also, epoxy is commonly used for developments of proof-of-concept of in photonic devices. However, while epoxy is an excellent choice for building up prototypes, its use in manufacturing should be assessed by experienced process and reliability engineers. Issues that should be reviewed include its:

- outgassing properties
- cure profiles (UV snap cure and thermal cure)

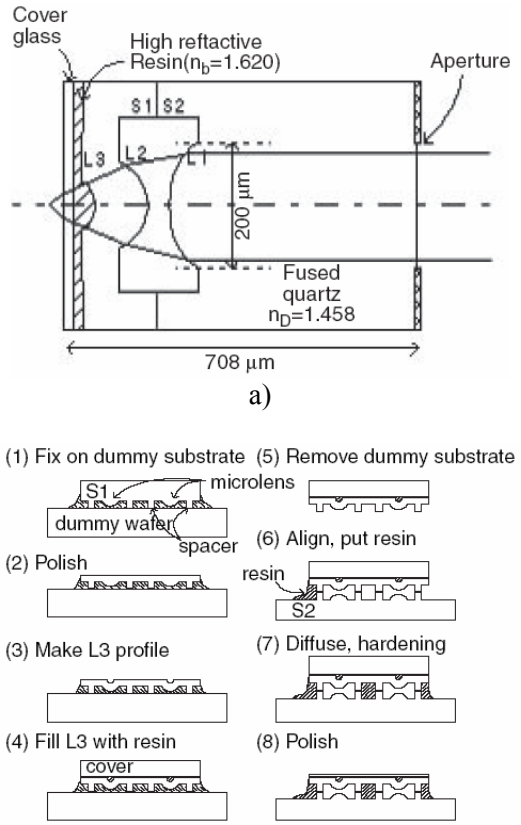

Figure 2.5. Structure of a high-NA microlens and its fabrication process flow [6].

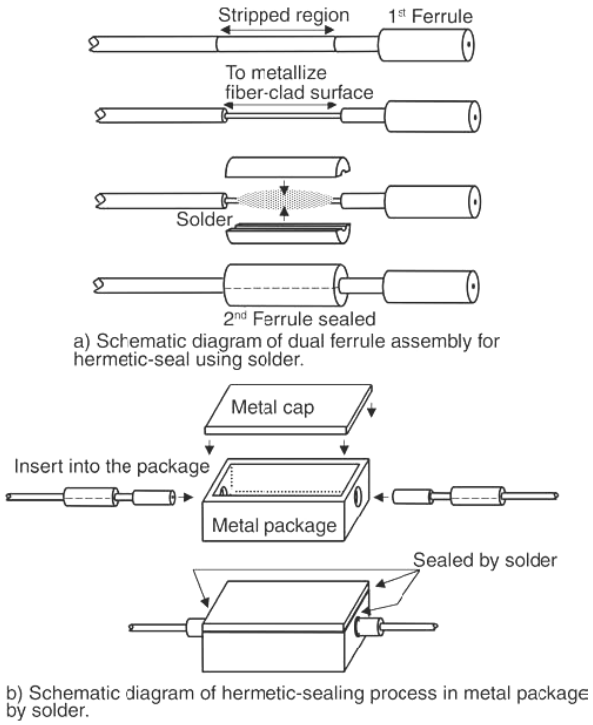

Figure 2.6. Hermetical sealing using soldering technique [6].

- shrinkage upon cure
- thermal expansion (CTE)
- mechanical stability
- adhesion strength
- refractive index and optical transmission in some applications
- ability to act as a reversible gas getter within thedevice package
- ability to maintain device optical coupling over Telecordia requirements
- processing cost relative to solder and laser weld attachment in a production environment

Positional shifts in epoxy attachments can degrade optical coupling in the device. These shifts can be caused by thermal cycling, due to material expansion, loss of adhesion, and changes in material properties due to environmental exposures such as humidity. The optical misalignment shifting can be a process-dependent function of epoxy volume, cure profile, and shape after cure. To diminish this problem, the use of UV snap cured or thermally cured epoxy is often required for precision alignment. The UV cured epoxy normally require the development of cure profiles that minimize both epoxy outgassing potential and component alignment shift. One more advantage of UV cured epoxies is its curing room temperature (fast none UC "snap cures" epoxy materials require 130˚ C to 160˚ C, [16].) Normally, the use of both thermally and UV snap cured epoxies minimize alignment shift of components when initially they are attached by UV snap cure.

The outgassing and stability of UV cured epoxies should be reviewed in detail to assess their compatibility with the photonic device in question (see reliability issues.) Table 1 shows general requirements of epoxy for optical fiber bonding.

3.4 Solder Attachment [16]

A common method used in holding photonic devices is solder attachment of submounts [Here, a distinction should be made between the use of solder attachment for mechanical structures such as submounts and the use of solder for attachment of pre-aligned optical components.] Often soldering processes for attachments require the use of flux. However, the use of flux requires special attention in the manufacture of photonic devices due to reliability concerns including contamination and cleaning process restrictions of many optoelectronic components. Therefore, a flux-less soldering process should be considered, since the removal of flux has shown significant thermal cycling life improvement when flux is thoroughly removed [16]. Figure 2.6 shows a sample process that utilizes soldering for hermetic sealing from [6].

- Ou *et. al* in [7] present a study of soldering optical fibers to V-grooves using a metallization technique including the use of Pb-free soldering. Electron-beam evaporation was used to deposit a multi-layered metallic coating on the surfaces of fibers and V-grooved chips to overcome the

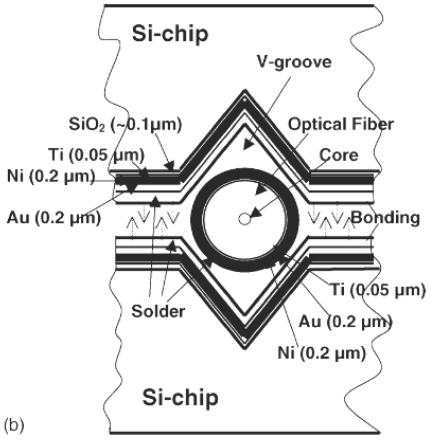

a)

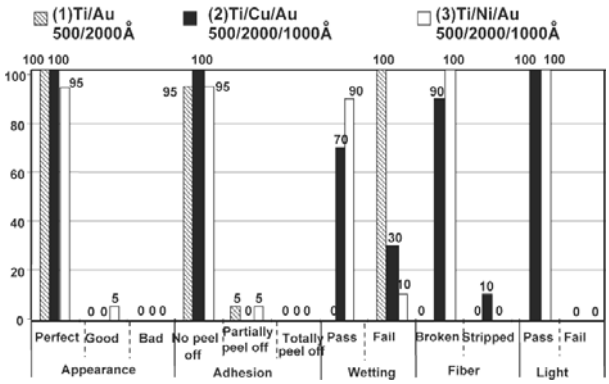

b)

Figure 2.7. a) Cross-section of the bonding structure, b) Pulling test results of three type of bonded surfaces via Pb-Free soldering [7].

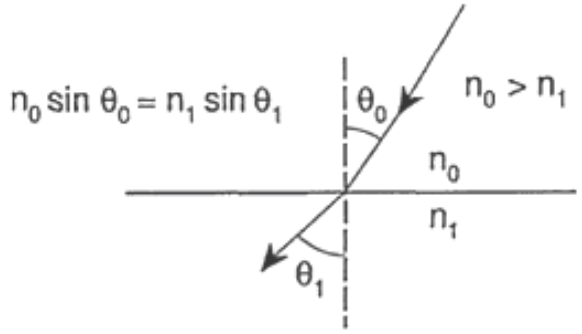

Figure A-1. Light refraction [22].

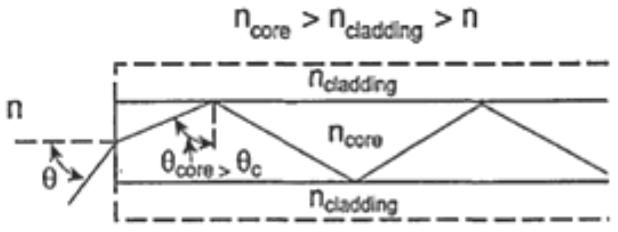

Figure A-2. Optical fiber showing the propagation of light through the core [21].

problem that solder does not wet the SiO_2 surface. Three types of coatings were investigated: Ti/Au, Ti/Cu/Au, and Ti/Ni/Au. These metallic film coatings have good adhesion on the fiber and the V-groove. Low melting point Pb-free solder was used, eutectic 43Sn-57Bi (in wt.%), with a melting point of 139 ˚C to bond an array of fibers to V-grooved chips.

Figure 2.7-a) show the coating layers used in their soldering technique, where precision alignment of fibers and the bonded structures were stable at room temperature. Figure 2.7-b) show bonding results for three type of soldering configurations, considering pulling tests including (Bellcore code GR-1221): adhesion, wetting, and appearance. The metallic solder bonding can be hermetic and it can isolate optical devices from ambient environment.

- In order to use proper solder attachment, components require compatible metal interfaces. Nickel/gold plating is often used to assure a good repeatable solder joint. Most ceramic substrates needing electrical connectivity have a metal surface layer compatible with the solder attachment. However, optical fibers, lenses and thin film filters require costly metallization processes, either require thin film metal evaporation deposition or by using electroless plating for metal adhesion to glass. For photonic package assembly, solder attachment may be successfully implemented by using the following processing tools and techniques [16]:

- by using a proper selection of solder joints, and a proper sequence of solder temperatures, solder joints would not reflow at subsequent assembly attachments. This can be alleviated by the increase of the subsequent solder reflow temperature by gold plating uptake into the solder during the beginning of solder reflow.
- by selecting a processing sequence allowing thorough solvent cleaning of soldered subassemblies before the integration of the sensitive optoelectronic components that can have their performance degraded due to solvent cleaning.
- by using cover gas belt furnaces or vacuum autoclave ovens. These two require the fabrication of special fixtures for the process.
- pre-tinning attachment surfaces, which can be solvent cleaned afterwards if desired, to improve the surface wetting capability of the solder and to reduce dependence on flux to ensure solder surface wetting.
- using no-clean fluxes, which do not affect the product's ability to pass Telcordia qualification requirements, that aid in solder surface wetting.

Optical components and fiber pigtails requiring precision attachment using solder requires special attention in setting up a process that achieves proper attachment position repeatability. Some process controls that allow solder attachment with high positional tolerances and repeatability include [16]:

- solder volume control

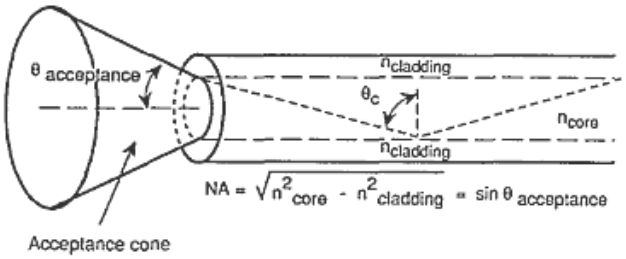

Figure A-3. Numerical aperture and acceptance angle [21].

- placement of solder volume, frequently resolved by employing solder preforms
- conditioning the solder preforms for optimal solder surface wetting by etching oxides off of preforms prior to use
- solder solidification shape
- application of a repeatable and controllable solder reflow temperature profile. The use of pulsed laser energy, resistance heating, and inductive heating are methods that can deliver such repeatable temperature profiles for solder attachment.

The use of laser soldering for attachment within photonic packages has an advantage because it is a contact-less heating method that can by far access the small components to be soldered that are hidden within small device packages. These recessed components are hard to access for resistance heating contacts and inductive heating coils. A good discussion on this matter is shown in [16].

4. Concluding remarks

This work first part of our work presents 1) general methods and processes for aligning and attaching optical fibers to a substrate, which considers direct aligning into silicon substrate, alignment through microlenses, connectors, optical waveguides, and hybrid approaches; 2) we also address critical issues concerning the development capability to align and package optical fibers with small elements. Issues such as tolerances, lateral and angular misalignments, and attachment methods are considered in this section. The critical issues related to insuring the reliability and stability of packaging over time and temperature are highlighted. The second report (Part II) of this investigation provides a development of alignment and assembly procedures of fiber optic assembly into Silicon chips.

Through highlighting the critical issues in the second part of this report, and covered the preliminaries of the assembly and fixation of optical fibers into micromachined substrates, we provide the state of the art of hybrid integration of Optical Fibers and MEMS.

Appendix

A1. Refraction, Total Internal Reflection, and Numerical Aperture [21]

As a ray of light crosses the boundary between two transparent media (e.g., air and glass), it is *refracted,* or bent. The amount of refraction, or bending, depends on the index of refraction *n* of ach material and on the angle of incidence θ. (For glass, *n* is approximately 1.5, and for air, *n= 1.0*.) Snell's law describes this relationship as

$$n_0 \sin\theta_0 = n_1 \sin\theta_1$$

where ***no*** = the index of refraction of the medium the light is traveling from

n1= the index of refraction of the medium the light is traveling to

θ_0= the angle between the incident ray and the normal to the surface

θ_1= the angle between the refracted ray and the normal to the surface

Figure A-1 shows the case where light is passing from a material of high index of refraction into a material with a lower index of refraction.

$$\theta_C = \sin^{-1}(n_1 / n_0)$$

One important measure of a fiber's ability to accept light is the numerical aperture, *NA*. It is dependent on the refractive of the core and cladding.

$$NA = \sqrt{n_{core}^2 - n_{cladding}^2}$$

Alternately,

Table A-1. Common fiber characteristics [22].

Fiber type	Mode	Core diameter (μm)	Cladding (μm)	Coating diameter (μm)	Refractive index delta	Numerical apertura	Max. Atten (dB/km)	BW-length (MHz-km)
50/125	multimode	50	125	250	1.0%	0.20	4.00[1]	500
662.5/125	Multimode	62.5	125	250	2.0%	0.275	3.75[1]	160
100/140	Multimode	100	140	250	2.2%	0.29	5.00[1]	100
8.3/125	Single-mode	8.3	125	250	0.37%	0.13	0.40[2]	NA[3]

$$NA = \sin \theta_{acceptance}$$

Where $\theta_{acceptance}$ is the acceptance angle shown in figure A-3.

A.2 Attenuation [21]

If power P_i is the optical power delivered to that part of the optical fiber following the inserted optical component, and P_o is the optical power delivered to that same part of the optical fiber before insertion of the optical component, then the attenuation or *insertion loss* is often given as a ratio in dB.

Attenuation = $-10 \log(P_o/P_i)$ dB

Where P_o = output power
P_i = input power, and
The units are in dB (decibels).
Light reflection [18])

$$\theta_C = \sin^{-1}(n_1 / n_0)$$

Typical fiber characteristics are shown in table A-1.

References

[1] "Second Edition of International Micro-Nano Roadmap," MANCEF - Micro and Nanotechnology Commercialization Education Foundation, 117 Bryn Mawr Drive SE #27 | Albuquerque, NM 87106 USA.

[2] Iliescu, C.; Jianmin Miao; Tay, F.E.H. "Low cost wafer level packaging of MEMS devices [piezoresistive pressure sensor example]" Electronics Packaging Technology, 2003 5th Conference, EPTC 2003, 10-12 Dec. 2003.

[3] Reichl, H.; Grosser, V. "Overview and development trends in the field of MEMS packaging" The 14th IEEE International Conference on Micro Electro Mechanical Systems, 2001. MEMS 2001.

[4] E. J. Palen "Taking a Photonic Device from Prototype to Manufacturing: Ten Common Pitfalls and How to Avoid Them" Proceedings from IEEE's Photonic Devices & Systems Packaging Symposium (PhoPack), Stanford University, California, July15th-16th, 2002.

[5] Mireles J., "Packaging Investigation and Study for Optical Interfacing of Micro Components with Optical Fibers" study developed for Sandia Natoinal Labs, document #9602, with PO# 659783. Applied Science and Technology Research Center, Universidad Autonoma de Ciudad Juarez, MX 2007.

[6] S. Kawai, Editor, "Handbook of Optical Interconnects," Taylor Francis 2005, ISBN: 0-8247-2441-0.[7] S. Ou, G. Xu, Y. Xu, K.N. Tu "Optical fiber packaging by lead (Pb)-free solder in V-grooves," Ceramics International 30 (2004) 1115–1119.

[7] Ou, G. Xu, Y. Xu, K.N. Tu, Ceramics International Vol. 30 Issue 7, (2004) p. 1115.

[8] S.-S. Lee, L.-S. Huang, C.-J. Kim, and M. C. Wu "2x2 MEMS Fiber Optic Switches With Silicon Sub-Mount For Low-Cost Packaging" Solid-State Sensor and Actuator Workshop Hilton Head Island, SC,. 1998

[9] L.-S. Huang, S.-S. Lee, E. Motamedi, M. C. Wu and C.-J. Kim "MEMS Packaging for Micro Mirror Switches," 1998 Electronic Components and Technology Conference, IEEE, pp. 592-597.

[10] D.C. Abeysinghe, V. Ranatunga, A. Balagopal, H. Mu, K. Ye, and D. Klotzkin "A Novel Technique for High-Strength Direct Fiber-to-Si Submount Attachment Using Field-Assisted Anodic Bonding for Optoelectronics Packaging," IEEE Photonics Technology Letters, Vol. 16, No. 9, Sep. 2004.

[11] G. Wu, A.R. Mirza, S.K. Gamage, L. Ukrainczyk, N. Shashidhar, G. Wruck and M. Ruda. Journal Of Micromechanics And Microengineering, **14** 1367 (2004).

[12] A. L. Glebov, M. G. Lee, and K. Yokouchi. Micro-Optics, VCSELs, and Photonic Interconnects II: Fabrication, Packaging, and Integration, Proc. of SPIE. **6185**, 618501. (2006).

[13] M. Karppinen, T. Alajokia, A. Tanskanena, K. Katajaa, J.-T. Mäkinena, P. Kariojaa, M. Immonenb, J. Kivilahtic, Micro-Optics, VCSELs, and Photonic Interconnects II: Fabrication, Packaging, and Integration, Proc. of SPIE **6185**, 61850O, (2006).

[14] M.S. Bakir, P.A. Kohl, A.L. Glebov, E. Elce, D. Bhusari, M.G. Lee, and J.D. Meindl, Photonics Packaging, Integration, and Interconnects VII, Proc. of SPIE **6478**, 647802, (2007).

[15] R. Hauffe, U. Siebel, K. Petermann, R. Moosburger, J-R. Kropp, F. Arndt, 2000 Electronic Components and Technology Conference, IEEE. (2000) p. 238.

[16] S. J. Adamson, J. J. Klocke, L. Nielson, Pori Engineering Conference 2001. (2001).

[17] T.Y. Lin, Optical Engineering **46**, 1 (2007).

[18] A. K. Nallani, T. Chen, D. J. Hayes, W.-S. Che, and J.-B. Lee, Journal of Lightwave Technology **24**, 1504 (2006).

[19] U. Gengenbach, Proceedings SPIE **2906**, 141 (1996).

[20] C. Lausch, R. Goering, F. Wippermann, MOEMS and Miniaturized Systems III, Proc. SPIE **4983**, 44, 0277-786X/03 (2003)

[21] [21] T.H. Buckle, Sandia National Laboratories Report SAND93-2478. Albuquerque NM, (1993).

[22] Y. G. Lee, S. K. Hong, M. Y. Park, S. C. Jung and S. H. Lee, MOEMS and Miniaturized Systems IV, Proceedings of SPIE Vol. 5346, (Bellingham, WA, 2004) p. 160.